Physics – Uspekhi **40** (2) 109 – 124 (1997)

REVIEWS OF TOPICAL PROBLEMS PACS numbers: **36.20.–r**, 61.25.Hq, **82.35.+t**, 82.70.Gg

Self-organization in ion-containing polymer systems

A R Khokhlov, E E Dormidontova

Contents

Abstract. A review is presented of theoretical and experimental studies on self-organization processes in ion-containing polymers (polyelectrolytes and ionomers). The high probability of various types of regular nanostructures in such systems is due to the effective competition between different interaction types, particularly the long-range Coulomb forces and hydrophobic interactions. The following self-organization phenomena in charged molecular systems are considered at some length: microphase separation in weakly charged polyelectrolyte solutions and gels in poor solvents; ordering in complexes of polyelectrolyte gels with oppositely charged surfactants; and formation of multiplet structures in ionomer systems.

1. Introduction

The results discussed in this review have arisen from the extension of research initiated by the works of I M Lifshitz. The development of the theory of coil – globule transition by I M Lifshitz [1 – 4] gave impetus to the search for other similar phenomena in polymer physics [5]. I M Lifshitz was in particular interested in such phenomena in polyelectrolyte systems and polymer gels. Both the design and the progress of early studies along these lines [6 – 10] used to be discussed in every detail with I M Lifshitz.

Ion-containing polymer molecules are those having charged units. A monomer link can be charged following dissociation which results in a charged unit and a low-molecular counterion. The number of counterions is equal to the number of charged units. As a rule, dissociation occurs when molecules are dissolved in highly-polar solvents, of which water is the most important (dielectric constant $\varepsilon \cong 81$). For this reason, by ionic polymer systems one mostly means the aqueous polymer solutions; in this case, a polymer coil may be schematically depicted as in Fig. 1a, with charged units and counterions being relatively independent of one another. The corresponding behavior of ion-containing macromolecules is called polyelectrolyte, and polymer chains are polyelectrolytes. An alternative behavior can be observed when counterions are condensed on oppositely charged monomer units of a polymer chain with the formation of the so-called ion pairs (Fig. 1b). Such behavior is known as ionomeric. It is realized in low-polarity media and will be discussed in detail in Section 5. Until then, we shall confine ourselves to the discussion of aqueous polyelectrolyte solutions (Sections 1 – 4).

Polyelectrolytes may carry both negative (polyanions) and positive (polycations) charges. Typical examples of anionic units frequently referred to in the forthcoming discussion are sodium acrylate (Fig. 2a) and sodium metacrylate (Fig. 2b). These units dissociate in the aqueous medium giving rise to a negatively charged group COO^- and an oppositely charged ion Na^+. An example of a cationic unit

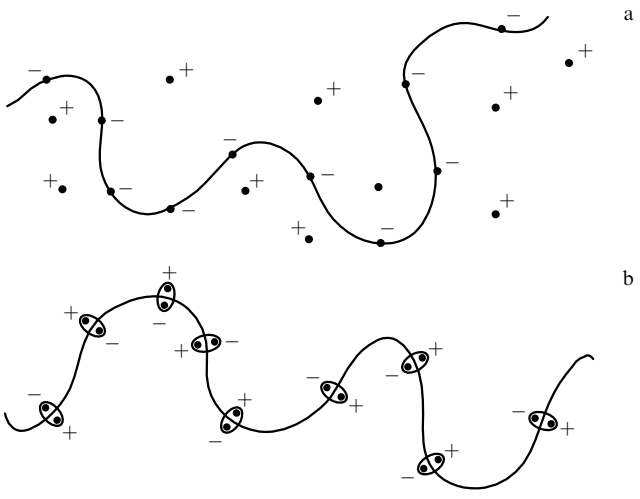

Figure 1. Polymer coil with charged units in the polyelectrolyte (a) and ionomeric (b) regimes. Dots are negatively charged monomer units and positively charged counterions.

A R Khokhlov, E E Dormidontova Physics Department, M V Lomonosov Moscow State University, Vorob'evy Gory, 119899 Moscow, Russia
Tel. (7-095) 939 10 13, 135 79 10
Fax (7-095) 939 29 88
E-mail: khokhlov@polly.phys.msu.su

Received 3 September 1996
Uspekhi Fizicheskikh Nauk **167** (2) 113 – 128 (1997)
Translated by Yu V Morozov; edited by A S Dobroslavskiĭ

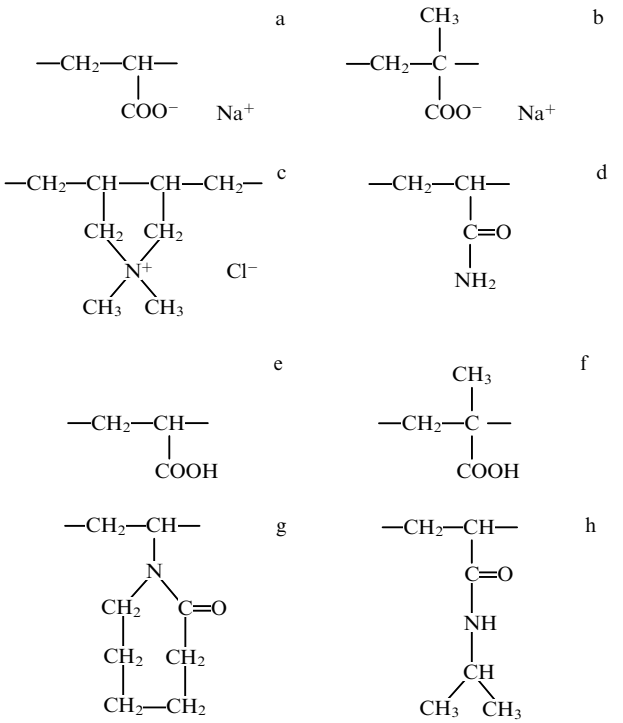

Figure 2. Structural formulas of monomer units of typical polymers cited in this review: sodium polyacrylate (a), sodium polymetacrylate (b), polydiallyldimethylammonium chloride (c), polyacrylamide (d), polyacrylic acid (e), polymethacrylic acid (f), poly-*N*-isopropylacrylamide (g), polyvinylcaprolactam (h).

is diallyldimethylammonium chloride (Fig. 2c) which dissociates releasing a counterion Cl^-. Polymer chains consisting merely of charged monomer units (like in Figs 2a – 2c) are called strongly charged polyelectrolytes.

The fraction of charged units can be smaller, e.g. in copolymers consisting of charged and neutral units (such as the acrylamide unit shown in Fig. 2d) or in chains with a pH-dependent charge (the monomer units of such well-known pH-dependent polymers as acrylic and metacrylic acids are presented in Figs 2e and 2f). The units shown in Figs 2e and 2f are not charged at low pH; however, they can acquire a charge at a higher pH (for instance these units can turn into anionic units (Fig. 2a, b) by the addition of alkaline NaOH; in this case, the fraction of charged units is controlled by the number of added alkaline molecules). Charged macromolecules with a small fraction of charged units are called weakly charged polyelectrolytes.

For strongly charged polymer chains, the long-range Coulomb interactions are of great importance. These interactions influence the system's behavior at the highest extent. For weakly charged electrolytes the effective competition between Coulomb and non-electrostatic interactions takes place. In aqueous systems, hydrophobic interactions [11] are the most important among the non-Coulomb ones. Hydrophobic interactions are due to the effective attractive forces between non-polar organic groups dissolved in water; the nature of these forces is related to the balance between the energy-dependent interactions of such groups with water and the entropy factors arising from the disintegration of the hydrogen bonds typical of water [11 – 13]. It is worthwhile to emphasize that hydrophobic attractive forces increase with temperature [12, 13].

The effective competition between Coulomb and hydrophobic interactions can take place not only in weakly charged polyelectrolytes but also in strongly charged ones provided their monomer units contain hydrophobic groups (e.g. CH_3-groups in polymetacrylic acid in Fig. 2f or sodium metacrylate in Fig. 2b). Therefore, such competition appears to be a universal property of polyelectrolyte systems.

Recent interest in systems exhibiting both Coulomb and hydrophobic interactions is connected with the fact that the competition between these two types of interactions leads to the formation of regular nanostructures in the form of ordered 1 – 100 nm microinhomogeneities. The presence of such regular microinhomogeneities in aqueous solutions of polyelectrolytes with hydrophobic interactions should be considered as a rule rather than an exception. The resultant nanostructures can have different morphology (hydrophobic spherical micelles, cylinders, lamellae, etc.) controlled by slight modulation of external parameters (concentration of an added low-molecular salt, pH, temperature, etc). This fact alone is sufficient to draw attention to such systems as being of interest both for fundamental research and for practical purposes.

There are two broad areas for potential practical application of polyelectrolyte systems with hydrophobic interactions. To begin with, the most important biological macromolecules, i.e. DNA and enzyme proteins, are polyelectrolytes. Their structure and biological functions are either directly determined by the balance of Coulomb and hydrophobic interactions (for proteins), or this equilibrium is essential for conformational transformations of biopolymers in the living cell (for DNA) [11].

Another field of potential applications of these systems is connected with the fact that ion-containing polymers always include charged polymer chains and counterions. Examples in Fig. 2 demonstrate that polymer chains have, as a rule, an organic nature whereas counterions (normally, Na^+ or K^+ for polyanions and Cl^- or Br^- for polycations) are the inorganic component. The presence of regular nanostructures of the polymeric component implies the regularity of the microinhomogeneous counterion distribution as well. Furthermore, ordinary polyelectrolyte counterions (Na^+, K^+, Cl^-, Br^-) can be replaced in the process of ion-exchange by more complex ones (e.g. ions of noble and rare-earth metals) which represent the inorganic component showing controlled regular microinhomogeneous distribution within the organic polymer matrix. Further reduction of metal ions to atoms allows obtaining regular metal nanostructures or nanoparticles in the polymer matrix. Such systems having the well-developed metallic surface with the controlled shape and size of microinhomogeneities are certainly of interest as catalysts with manageable activity. One more area of the potential application of these systems is the production of nanocomposite materials of the metal – polymer or semiconductor – polymer types.

The present review summarizes theoretical and experimental data on self-organization process leading to regular nanostructures in ion-containing polymer systems. Namely, the microphase separation in weakly charged polyelectrolytes and polyelectrolyte gels in poor solvents (Section 3), ordering in polyelectrolyte gel complexes with oppositely charged surfactants (Section 4), and multiplet structure formation in ionomer systems (Section 5) are considered. Since a large part of Section 3 and all Section 4 are concerned with polyelectrolyte gels, it would be reasonable to start with a brief review

of the main physical effects related to gel swelling in water (Section 2).

2. Swelling and collapse of polyelectrolyte gels

Schematic representation of a polyelectrolyte gel is shown in Fig. 3. It consists of polyelectrolyte molecules cross-linked by covalent chemical bonds into an integrated spatial carcass swelling in a solvent (usually in water). Gels of the linear size of 1 mm to 1 cm are normally used in experiments, although microgels of down to 100 nm are feasible. The gel as a whole is actually one giant three-dimensional molecule.

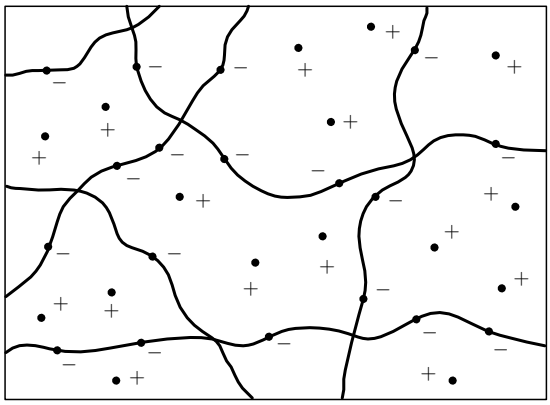

Figure 3. Schematic representation of polyelectrolyte gel swollen in a solvent. Dots are negatively charged monomer units and positively charged counterions.

An advantage of studying gels instead of linear macromolecule solutions is the possibility of direct visual recording of conformational changes in polymer chains resulting in the change of macroscopic gel size. The main disadvantage is the long period of time necessary for the equilibrium in macroscopic gel sample to be achieved (several days for gels a few centimeters in size). However, the corresponding characteristic time τ can be reduced by changing the size of the sample since it is connected with the process of solvent diffusive penetration into the gel,

$$\tau \propto L^2, \tag{1}$$

where L is the linear size of the gel sample.

Figure 3 shows that a polyelectrolyte gel contains counterions together with charged monomer units which ensures the electoneutrality of macroscopic gel sample as a whole. When a gel is swelling in a large volume of water, it appears advantageous for the counterions to abandon the network and pass into the surrounding solution because it would lead to a substantial translational entropy gain. However, this is not the case since the principle of electroneutrality of macroscopic gel sample would be violated. So, the counetrions have to remain inside the network where they produce expansive osmotic pressure. This pressure is responsible for the two most important physical effects taking place in polyelectrolyte gels swelling in water.

Firstly, a simple theory [10, 14, 15] shows the presence of a very strong effect of the osmotic pressure resulting in the considerable gel swelling in water: one gram of dry polymer may consume several kilograms of water absorbed by the gel. This allows polyelectrolyte gels to be used as the so-called superabsorbents of water (diapers, retention of soil moisture, dust immobilization, etc).

Secondly, excessive swelling of polyelectrolyte networks in water explains their sharp contraction upon deterioration of solvent quality leading to a thousand-fold jumpwise decrease in the gel volume. This phenomenon called gel collapse was first theoretically predicted in Ref. [16] and experimentally observed in Ref. [17]. It is connected with the coil – globule transition [3, 4] in polymer chains of a gel which accounts for the collapse of a gel as a whole. The stronger the charge of the gel, the sharper the collapse [14]. This is easy to understand in terms of the gel collapse theory developed in Refs [10, 14, 18, 19], according to which the collapsed phase is stabilized by the attractive forces between uncharged units. In this case, the gel volume displays weak charge dependence, whereas the volume of swollen gel grows considerably with increasing charge due to osmotic pressure of counterions.

3. Microphase separation in weakly charged polyelectrolyte systems in poor solvents

After the experimental discovery of polymer gel collapse and the development of a theory of this phenomenon, it became a matter of growing interest as an example of the abrupt cooperative conformational transition caused by slight variation of external conditions [19, 20]. This even gave rise to the term 'responsive gels' referring to polyelectrolyte networks [20]. It has been shown that gel collapse can be induced not only by the addition of a poor organic solvent but also by adding low-molecular salts [21, 22], surfactants [23, 24] or polymers [25, 26] to the external solution, by changing pH and temperature [28, 29], etc.

Below we will concentrate our attention mainly on the cases when gel collapse is induced by a change of temperature in pure aqueous media. This is the case with poly(*N*-isopropylacrylamide) (PNIPA) and polyvinylcaprolactam (PVC) networks whose repeating units are shown in Figs 2g and 2h, and also with copolymers of these units containing charged monomer links (Figs 2a – 2c). PNIPA and PVC gels are thermosensitive; they readily swell in water at room temperature but collapse at elevated temperature (between 30° and 40 °C) [28, 29]. This can be accounted for by the presence of both polar (water-soluble) and non-polar (hydrophobic) groups in the monomer units shown in Figs 2g and 2h. Enhanced hydrophobic attraction between non-polar groups with increasing temperature leads to gel collapse. In accordance with the general theory [14, 19], the collapse becomes more sharp and its 'amplitude' increases [29] when neutral thermosensitive units copolymerize with charged ones (Figs 2a – 2c).

Collapse of gels based on PNIPA – sodium acrylate copolymers has been studied in detail in Ref. [30]. The authors observed swelling of these gels in heavy water and studied the resultant structure by the small-angle neutron scattering technique. Fig. 4 shows the dependence of scattering intensity on the wave vector at different temperatures for a gel containing 5% of charged sodium acrylate units. Evidently, a temperature rise results in a progressively growing maximum on the plot. Now, the peak on a small-angle scattering curve at the finite wave vector q_0 suggests the appearance of the characteristic spatial period $\lambda = 4\pi/q_0$ of polymer density fluctuations in the system, i.e. a trend to the formation of a microdomain structure with such spatial period. The common picture is rather similar to that of the so-called

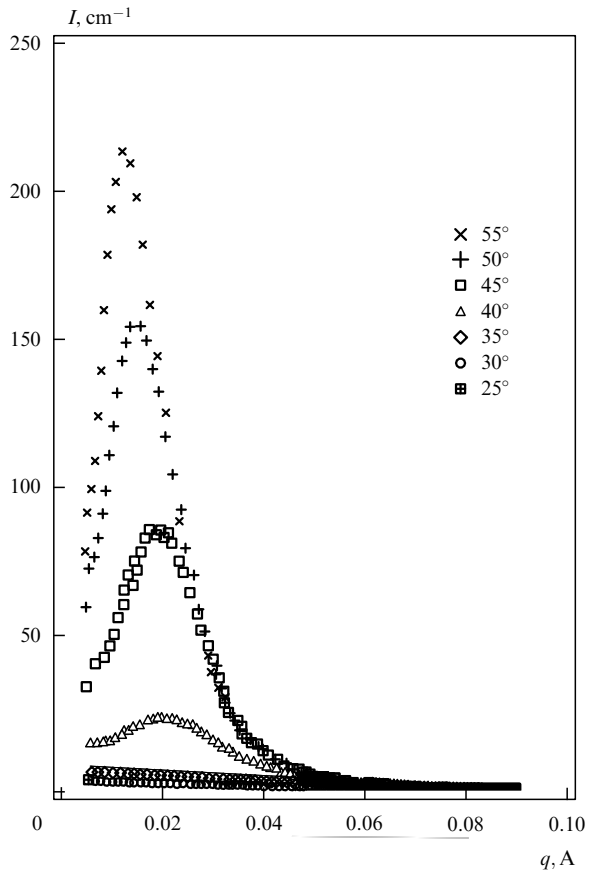

Figure 4. Intensity of small-angle neutron scattering vs the wave vector for PNIPA – sodium acrylate copolymer gels swelling into heavy water at different temperatures (from [30]).

microphase separation well studied for block-copolymer systems [31 – 33]. Because of this, the effect under consideration was called microphase separation in weakly charged polyelectrolyte gels [30].

Figure 4 shows the apparent maximum on the small-angle scattering curve as early as the temperature reaches 40 °C when the gel remains essentially swollen. This means that the observed microphase separation is not directly connected with gel collapse.

Similar results have been obtained by another group [34, 35] who studied (by small-angle neutron scattering technique) the microstructure of weakly charged polyacrylic acid gels collapsing in heavy water.

How can the observed effect be explained theoretically? A relevant theory had actually been suggested by Erukhimovich and Boru [36, 37] a few years before the experimental observations, an excellent example of theoretical predictions come true. On qualitative level, the main result of Refs [36, 37] as applied to collapsing polymer gels may be described in the following way (Fig. 5).

Let us consider a weakly charged polyelectrolyte gel in the solvent, the quality of which (for uncharged units) is slowly deteriorating (which corresponds to a temperature rise for thermosensitive PNIPA units). Then the gel tends to collapse. However, a sharp decrease in its volume, and hence in the volume in which the counterions occur, leads to a substantial loss of their translational entropy. Another possibility is the formation of a microstructure (see Fig. 5) in which aggregates of uncharged hydrophobic units alternate with grossly swollen regions containing the majority of charged units and

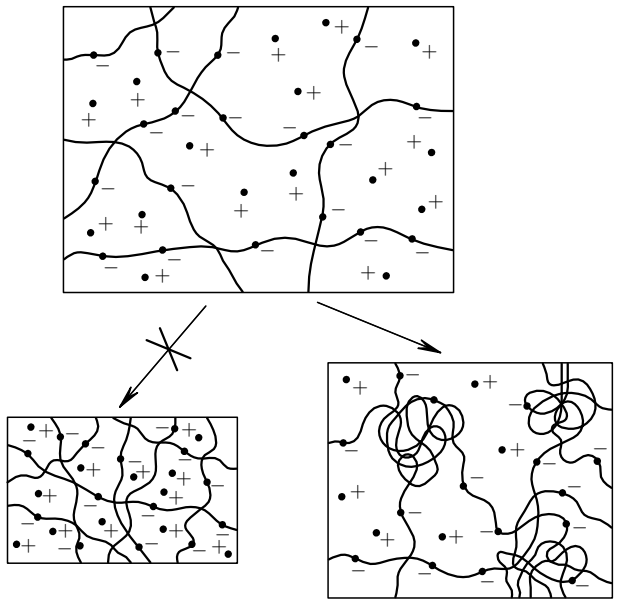

Figure 5. An illustration of the possibility of microphase separation in a weakly charged polyelectrolyte gel in a poor solvent.

counterions. The number of disadvantageous contacts between uncharged units and water considerably decreases without significant change in the gel volume (i.e. without a change in the osmotic pressure produced by counterions). In other words, the microstructure can arise even in a swollen gel, in perfect agreement with experimental data [30].

It is worthwhile to note that the initial theoretical prediction [36] was concerned with a polyelectrolyte solution in a poor solvent rather than a polymer gel, although similar arguments can be applied to both situations. It was shown later that microphase separation is a universal feature of polyelectrolyte systems, and occurs in all systems showing competing trends to component segregation at smaller scales and stabilization by the long-range factor of Coulomb nature which inhibits formation of large-scale inhomogeneities. Thus, the microphase separation has been studied in mixtures of weakly charged polycations and polyanions having incompatible uncharged units [38, 39], mixtures of charged and neutral polymers [40, 41], and mixtures of two likely charged polyelectrolytes with different amount of charge, for polyelectrolyte solutions in poor solvents [42].

Let us consider the initial theoretical expression for the free energy F of a mixture of two weakly charged polyelectrolytes A and B dissolved in the same solvent S which allows analyzing the advantage of microphase separation in such a system. To this end, the free energy must be written for the microinhomogeneous state in which the volume fractions of components Φ_A, Φ_B, and Φ_S are functions of the spatial coordinate $\mathbf{r}$. Then, the expression

$$\frac{F}{kT}=\frac{1}{b^3}\int \mathrm{d}^3r\left\{\frac{\Phi_A}{N_A}\ln\Phi_A+\frac{\Phi_B}{N_B}\ln\Phi_B+\Phi_S\ln\Phi_S\right.$$
$$+\chi_{AB}\Phi_A\Phi_B+\chi_{AS}\Phi_A\Phi_S+\chi_{BS}\Phi_S\Phi_B+\sum_i n_i\ln n_i$$
$$\left.+\frac{l_A b}{24}\frac{\left(\nabla\Phi_A^{1/2}(\mathbf{r})\right)^2}{\Phi_A}+\frac{l_B b}{24}\frac{\left(\nabla\Phi_B^{1/2}(\mathbf{r})\right)^2}{\Phi_B}\right\}$$
$$+\frac{1}{2\varepsilon kT}\iint \mathrm{d}^3r\,\mathrm{d}^3r'\,\frac{\rho(\mathbf{r})\rho(\mathbf{r}')}{|\mathbf{r}-\mathbf{r}'|} \qquad (2)$$

is written in the approximation of the Flory–Huggins lattice model which suggests that both monomer units A and B and molecules of solvent S fill the same lattice cell of volume $v = b^3$, and the component interactions are determined by the Flory–Huggins constants χ_{AB}, χ_{BS}, and χ_{AS} [43, 15]. The following notation is used: T is the temperature, k is the Boltzmann constant, N_A and N_B are the numbers of units in chains A and B respectively, l_A and l_B are the Kuhn segment lengths of these chains, $n_i(\mathbf{r})$ is the concentration of low-molecular ions of type i at point $\mathbf{r}$, ε is the dielectric constant of the solvent, and

$$\rho(r) = e\left[\sum_i z_i n_i(\mathbf{r}) + \frac{1}{v} z_A f_A \Phi_A(\mathbf{r}) + \frac{1}{v} z_B f_B \Phi_B(\mathbf{r})\right] \quad (3)$$

is the volume charge density at point $\mathbf{r}$. In the expression (3), e is the elementary charge, z_i, z_A, and z_B are the valencies of low-molecular unit of type i, charged units in chains A and B respectively, f_A and f_B are the fractions of charged units in chains A and B.

The first three terms of the functional (2) describe the translational entropy of the chains and the effects of the excluded volume, the following three terms represent non-Coulomb interactions between the components, the next term is the contribution of translational entropy of the low-molecular ions, and the following two ones — the entropy loss due to the non-uniform distribution of the concentrations of polymers A and B (Lifshitz entropy [1–4]). The last item is the contribution of Coulomb interactions. Only two of the three functions $\Phi_A(\mathbf{r})$, $\Phi_B(\mathbf{r})$, and $\Phi_S(\mathbf{r})$ in the expression (2) are independent because the following incompressibility condition is valid:

$$\Phi_A(\mathbf{r}) + \Phi_B(\mathbf{r}) + \Phi_S(\mathbf{r}) = 1\,. \quad (4)$$

Furthermore, the functions $n_i(\mathbf{r})$, $\Phi_A(\mathbf{r})$, and $\Phi_B(\mathbf{r})$ are connected by the Poisson–Boltzmann equation [44]. The linearized form of the equation (i.e. reduced to the Debye–Hukkel form [41]) is, however, unacceptable for description of microdomain structures.

Taking into consideration all these relations between the functions, the functional (2) should be minimized over all possible distributions $\Phi_A(\mathbf{r})$, $\Phi_B(\mathbf{r})$, and $n_i(\mathbf{r})$ to obtain the distribution corresponding to the free energy minimum. The solution of this problem in the general form encounters serious mathematical difficulties; so the task has been completely solved only for a few specific cases.

For example, Fig. 6 presents the phase diagrams obtained in Ref. [41] by direct minimization of the free energy (2) for a mixture of neutral (B) and charged (A) polymers with $N_A = N_B = 10^3$ and the charged units fraction $f_A = 0.01$ for three values of the parameter τ which characterizes the dielectric properties of the medium. The minimizing procedure in [41] took into account only the formation of a lamellar microdomain structure. The hatched area in Fig. 6 is the stability region of microphase separation, while the dotted area corresponds to macrophase separation region. It can be seen that the stability region of the microdomain structure is actually an island inside the region of macroscopic phase separation. So, with an increase of the incompatibility parameter χ, the microdomain structure appears in one of the two coexisting macroscopic phases. Also, it is worthwhile to note that the stability region of the microdomain structure grows with the increase in the dielectric constant of the medium.

The period of the lamellar microdomain structure λ, as estimated in Ref. [41], turned out to be normally equivalent to 50–200 characteristic unit sizes. i.e. several tens of nanometers. Hence, the arising microinhomogeneities may be considered as regular nanostructures.

In Ref. [42], the problem of computation of the phase diagram and characteristics of the arising microdomain structures for solutions of weakly charged polyelectrolytes in poor solvents was solved entirely in the so-called weak

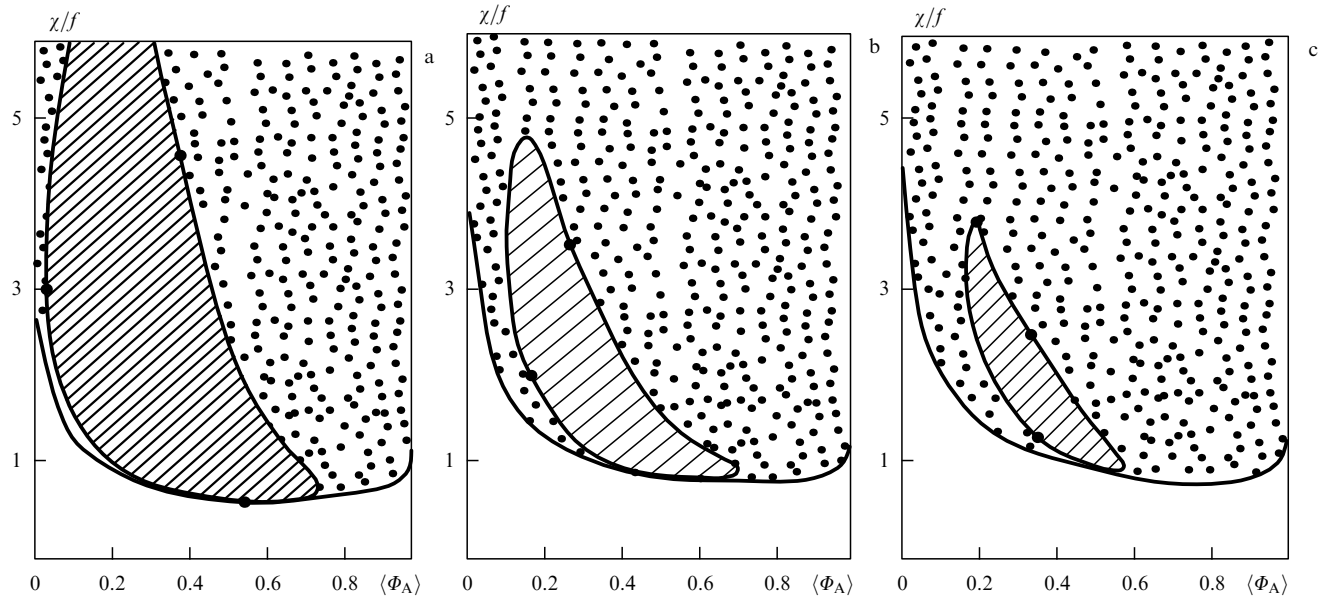

Figure 6. Phase diagrams for a mixture of neutral (B) and charged (A) polymers with charged unit fractions $f_A = 0.01$; $N_A = N_B = 10^3$; Flory–Huggins parameter χ, three values of the dimensionless parameter: $\tau = 4\pi e^2/\varepsilon kTa = 1$(a), 3 (b), 4 (c) [41]. The hatched area is the region of thermodynamic stability of lamellar microdomain structure. The dotted area is the region of separation into two macroscopic phases. $\langle\Phi_A\rangle$ is the mean volume fraction of polymer A.

segregation approximation which implies expansion of a free energy functional [like that in Eqn (2)] in powers of polymer and counterion concentration fluctuations. This approximation is valid near the spinodal of microphase separation [31, 32]. Figure 7 shows a phase diagram obtained in Ref. [42] for the salt-free weakly charged polyelectrolyte solutions. The diagram is plotted in variables: polymer – solvent interaction parameter, χ, mean volume fraction of polymer in the solution $\langle\Phi\rangle$. The diagram contains the stability regions of homogeneous phase (*1*), body-centered-cubic phase of spherical hydrophobic micelles (*2*), hexagonal phase of cylindrical hydrophobic micelles (*3*), and lamellar phase with alternating hydrophobic and grossly swollen layers (*4*), as well as the region of macroscopic phase separation into two phases.

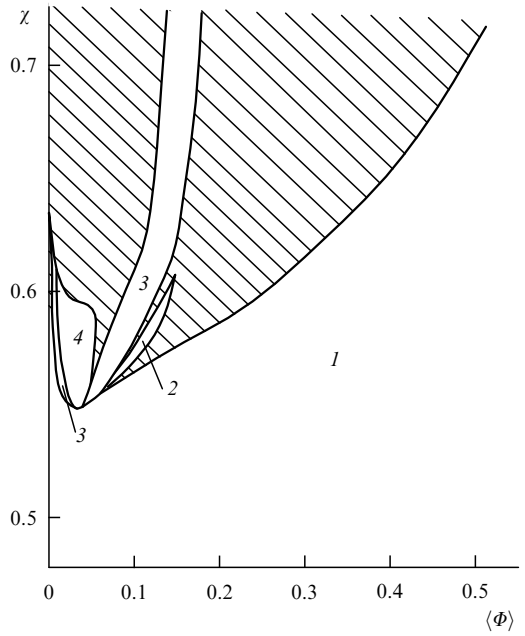

Figure 7. Phase diagram for a salt-free solution of weakly-charged polyelectrolyte in a poor solvent for $\tau = 4\pi e^2/\varepsilon kTa = 4$ [42]. The diagram contains the regions of stability of homogeneous phase (*1*), body-centered cubic structure of spherical micelles (*2*), hexagonal structure of cylindrical micelles (*3*), and lamellar phase (*4*), as well as the region of macrophase separation (hatched area). χ is the polymer – solvent interaction parameter, $\langle\Phi\rangle$ is the mean volume fraction of polymer in the solution.

It is clear that the main qualitative properties of this phase diagram coincide with those of the diagram in Fig. 6, viz. the microdomain phases of different morphology are stable in the 'islands' inside the zone of macroscopic phase separation; microdomain structures arise with increasing χ in one of the coexisting phases as a result of macrophase separation. The period of the structure is of the order of several tens of nanometers, similar to that in a polymer mixture.

The principal experimental results of Refs [30, 34, 35] concerning the microdomain structure period, its dependence on the polymer concentration, the added salt, and the charged unit fraction are in agreement with the theory developed in Refs [36 – 42]. However, the experiments largely involved polyelectrolyte networks whereas the theory is concerned with solutions and mixtures of linear macromolecules. This discrepancy was overcome in a recent study [45], where the above theory [36 – 42] was generalized for poor solvent polyelectrolyte gels. The assembly of macromolecules into the gel network was taken into account by adding a phenomenological term to the free energy (2) suggested by De Gennes [46] which reflects the impossibility for monomer units of a given subchain (between two cross-links) to occur far from the network cell to which this subchain belongs. Moreover, to generalize the technique of microphase separation studies to polyelectrolyte gels, it is necessary to take into account that the volume of the polymer system (gel) is not fixed in this case and should be deduced from the condition of zero osmotic pressure [17].

Figure 8 shows a calculated collapse curve [45] which describes the dependence of the mean polymer volume fraction in a network $\langle\Phi\rangle$, (this value is inversely proportional to the total gel volume V), on the polymer – solvent incompatibility parameter χ. This dependence is obtained for the case of a gel in which 6% of the units are charged and the number of units in a subchain between two cross-links is 1000. In this case, gel contraction is a multistage process, by contrast to the classical collapse picture. Indeed, as the properties of the solvent deteriorate, the gel first undergoes transition from the ordered swollen phase to the intermediate phase with microdomains of lamellar symmetry; then the volume changes again, with the simultaneous morphological transformation of microdomain structures to hexagonal phase with hydrophobic cylindrical micelles. Finally, the last jump of the volume results in the disordered collapsed phase. The period of the microdomain structure in intermediate phases with non-trivial morphological features is invariably 15 – 20 unit sizes, i.e. around 10 nm. Figure 8 shows that the region of collapse contains also numerous metastable phases in addi-

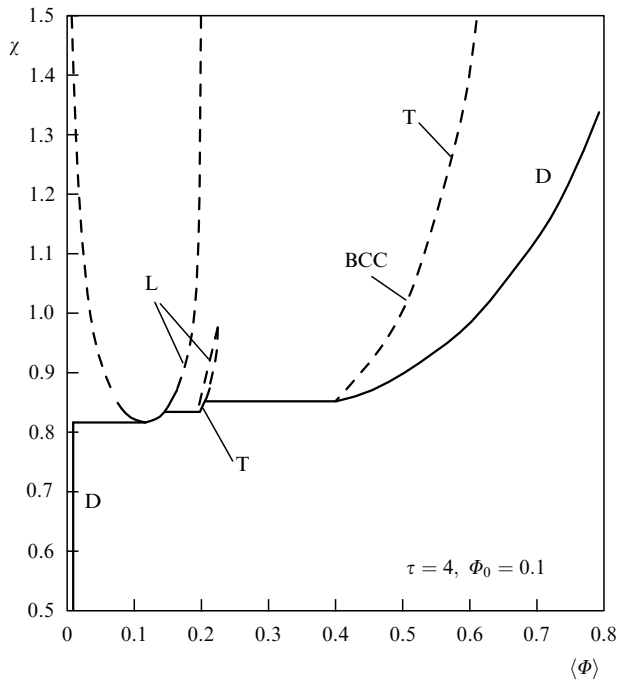

Figure 8. Dependence of the mean polymer volume fraction $\langle\Phi\rangle$ on the polymer – solvent incompatibility parameter for a polyelectrolyte gel with the charged unit fraction 0.06, the number of monomer units in a subchain between two cross-links 1000, $\tau = 4$, and the volume fraction of the polymer at the synthesis conditions 0.1. The solid line is the equilibrium collapse curve, different dashed lines show metastable states with morphologically different microdomain structures (L — lamellar phase, T — triangular phase, BCC — body-centered cubic phase, D — disordered phase).

tion to those mentioned above, which accounts for the possibility of hysteresis associated with non-monotonic changes of the parameter χ.

Thus, according to Ref. [45], the possibility of the existence and stability of morphologically different microdomain phases in collapsing polyelectrolyte gels can result in multistage gel collapse accompanied by microphase separation at intermediate stages. In this case, conformational transition in a polyelectrolyte gel is likely to be accompanied by hysteresis. These theoretical results are in good agreement with recent experimental data [47] where both intermediate phases and hysteresis were observed.

4. Ordering in polyelectrolyte gel complexes with oppositely charged surfactants

Complexes of charged polymer gels with oppositely charged surfactants provide another example of polyelectrolyte systems giving rise to regular nanostructures. Such complexes were first examined in a theoretical study [24] and in macroscopic experiments [23, 48, 49]. The most important qualitative results obtained in Ref. [24] are presented below.

Let us assume that a polyelectrolyte gel is swelling in a large volume of a diluted oppositely charged surfactant solution (Fig. 9a), and surfactant concentration is much lower than its critical micelle concentration (CMC). Such a system has an additional degree of freedom as compared with the one swelling in pure water: the ion exchange between gel counterions and surfactant ions in the external solution is possible. If the volume of the external solution is sufficiently large, the ion exchange may result in the replacement of practically all counterions by surfactant ions (Fig. 9b). It can be concluded that in the situation shown in Fig. 9, the surfactant molecules are effectively absorbed by the gel; hence, their concentration inside the network may easily exceed CMC and micelle formation can occur.

Micelle formation is also promoted by the fact (first observed in Ref. [24]) that a CMC inside the gel is much lower than in the external solution. The theory of this effect has been developed in Ref. [24]. It can be described in the qualitative language in the following way. A micelle being formed in the aqueous solution (Fig.10a) acquires a large charge which is partially compensated by the accumulation of surfactant counterions around the micelle. This results in substantial immobilization of counterions, disadvantageous in terms of entropy. Conversely, when a micelle is formed inside the network (Fig. 10b), its charge is neutralized by the initially immobilized gel charges which do not possess translational entropy. Therefore, in this case the loss of entropy associated with the micelle formation is significantly smaller, leading to a substantial CMC decrease as in the situation shown in Fig. 10b.

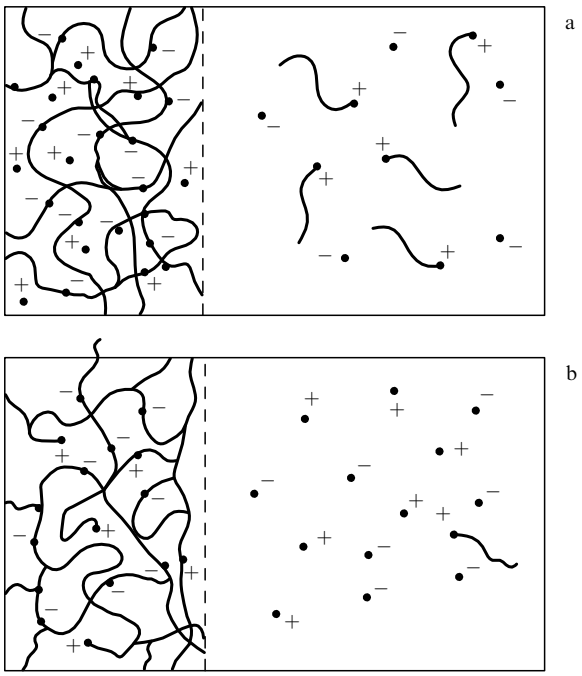

Figure 9. Polyelectrolyte gel is placed into a dilute solution of oppositely charged surfactants (a); this results in the replacement of counterions by surfactants (b). Surfactant molecules are depicted as short hydrophobic chains with charged end-unit.

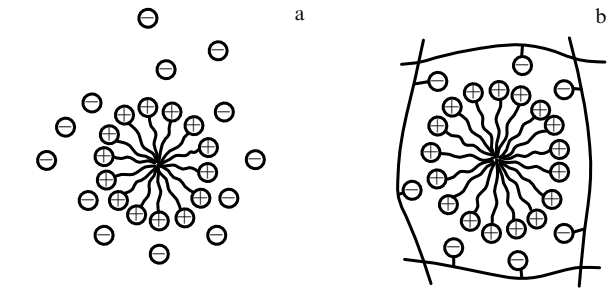

Figure 10. Surfactant micelle in aqueous solution (a) and in gel (b).

Theoretical analysis of [24] has demonstrated that the organization of surfactants into micelles inside the gel leads to a significant reduction of counterion pressure and the collapse of the gel. The collapsed complex gel – oppositely charged surfactant has the charge ratio 1:1 and contains hydrophobic microregions due to the aggregation of surfactant tails. Therefore, the complex should be able to absorb small admixtures of water-soluble organic molecules.

The predictions of the theory suggested in Ref. [24] were confirmed by experiments on a variety of polyelectrolyte gel – oppositely charged surfactant complexes reported in Refs [23, 29, 49 – 53]. Gels used in the experiments included homo and copolymers of practically all monomer units shown in Figs 2 and 5, viz polycations and polyanions, strongly and weakly charged gels, thermosensitive and insensitive monomer units. Major oppositely charged surfactants were anionic ones for cationic networks (sodium alkylsulfates, see Fig. 11a for the chemical structure), and cationic ones for anionic networks (alkylpyridinium chloride, Fig. 11b).

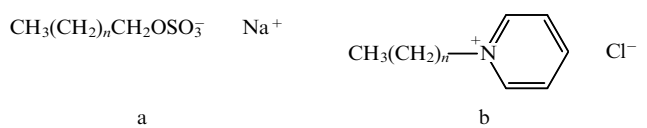

Figure 11. Structural formulas of surfactants: sodium acrylsulfate (a) and acrylpyridinium chloride (b). The number of carbon atoms in the hydrophobic tail n may vary.

Similar results were obtained for all gel – oppositely charged surfactants pairs. Figure 12a presents some data reported in Ref. [23] (decreased gel mass due to surfactant addition as a function of the molar ratio γ of the added surfactant to gel charges). For both cationic gel – anionic surfactant and anionic gel – cationic surfactant complexes, the gel undergoes sharp contraction as surfactants are added. On the other hand, the collapse is described in these coordinates by a continuous curve showing no apparent leap.

Figure 12b shows that all surfactant molecules are actually absorbed by the gel. This figure demonstrates γ-dependence of surfactant distribution coefficient between the gel and the external solution (i.e. the ratio of surfactant concentrations in gel and external solution) for anionic networks interacting with cetylpyridinium bromide [23]. These surfactant molecules have the absorption band in the UV region which allows to measure directly their concentration with a spectrophotometer. Evidently, when the optimal amount of surfactant molecules is added to the gel, the internal to external surfactant concentration ratio is about four orders of magnitude, confirming that the surfactant is really absorbed by the gel. No wonder, such a high surfactant concentration inside the gel facilitates the organization of surfactant molecules into micelles.

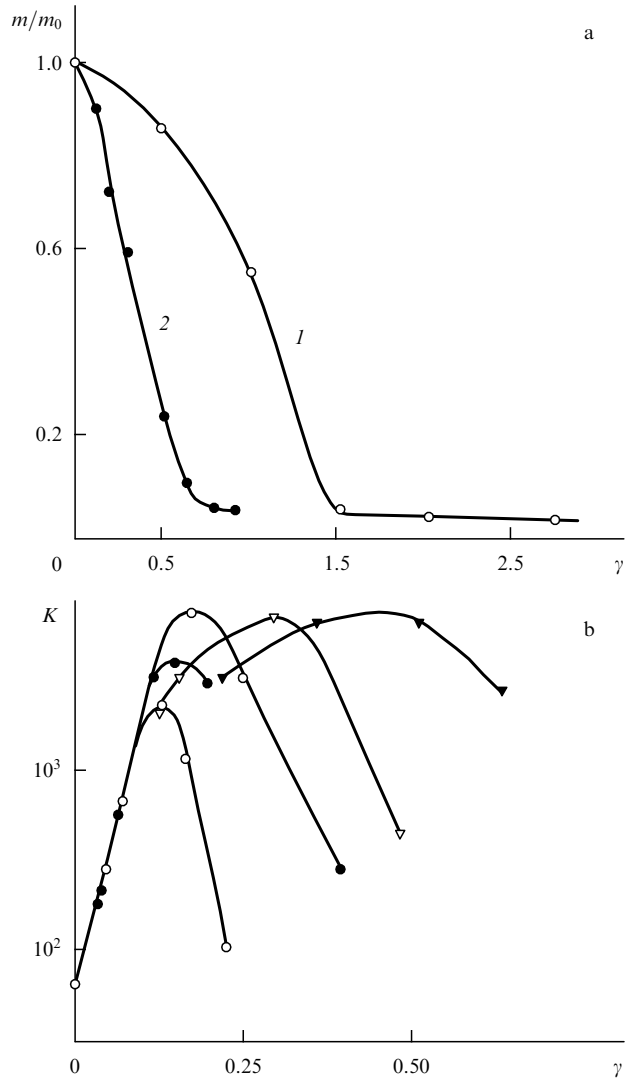

Figure 12. (a) A decrease in the polyelectrolyte gel mass m as oppositely charged surfactants are added. m_0 is the mass of the gel swollen in an aqueous solution, γ is the molar ratio of the number of added surfactant molecules to that of charged monomer units of the network. Curve *1* — cationic gels of diallyldimethylammonium bromide interacting with sodium dodecylsulfate, curve *2* — anionic sodium metacrylate-based gels interacting with cetylpyridinium bromide. (b) Distribution constant of cetylpyridinium bromide molecules in complexes with anionic sodium metacrylate-based gels (i.e. the ratio of surfactant concentration inside and outside the gel) as a function of the molar ratio γ of the number of added surfactant molecules to that of charged monomer units of the network. Different curves correspond to different charged unit fractions in the gel.

Intensive absorption of water-insoluble dyes [48] and phenols dissolved in a small amount of the external solution [54] provides indirect evidence of the presence of micelles (or hydrophobic aggregates) inside the gel. The table shows the distribution coefficients for phenols (i.e. the ratios of phenol concentration in the gel and in the external solution) and the percentage of absorbed molecules in the case when the sorbent is a complex of diallyldimethylammonium bromide gel and oppositely charged potassium salts of fatty acids differing in the length of hydrophobic tails. The experiments were carried out at one mole of charged cationic groups of the gel per 400 l of water, at room temperature. It is clear that the organic molecules of phenols are actually absorbed by gel – surfactant complexes which is only possible if these complexes contain surfactant hydrophobic aggregates.

Table. Fraction of absorbed phenol molecules and gel – water partition constants K (400 l per one mole of gel cationic groups) for complexes of DADMAB – potassium salts of fatty acids with different length of hydrophobic tail.

Phenol	Pyrogalol		Gallic acid		Tetrachloro-guaiacol		α-naphthol	
Surfactant	%	*K*	%	*K*	%	*K*	%	*K*
$C_{11}H_{23}$	93	1040	99	13000	86	220	–	–
$C_{13}H_{27}$	92	450	99	3200	69	50	72	210
$C_{17}H_{35}$	96	800	99	2800	80	130	75	80

Ref. [49] reports the direct measurement of the surfactant concentration at which micelle formation occurs (i.e. CMC inside the gel) in complexes of cationic gel (diallyldimethylammonium bromide) and oppositely charged surfactant (sodium dodecylsulfate). To this effect, fluorescence spectra of pyrene molecules, hydrophobic organic fluorescent probes, were obtained to estimate the degree of hydrophobicity in the vicinity of the probes. At surfactant concentrations below CMC, these molecules are largely surrounded with water, and their fluorescence spectra correspond to curve *1* in Fig. 13a. When pyrene concentration is higher than CMC, the molecules are mostly accumulated inside the hydrophobic micellar core, i.e. their environment becomes hydrophobic and the fluorescence spectrum changes as illustrated by curve *2* in Fig. 13a. The degree of hydrophobicity can be estimated from the characteristic peak intensity ratio I_3/I_1 in the fluorescence spectrum, and also from the appearance of a new excimer maximum at ~ 470 nm. Figure 13b shows the I_3/I_1 ratio as the function of added surfactants concentration. It appears to change considerably, at $C^* = 5.5 \times 10^{-4}$ mol l^{-1}, from the value characteristic of the pure aqueous milieu of pyrene molecules to a significantly higher value suggesting enhanced hydrophobicity of the surrounding medium. Therefore, C^* should be identified with CMC in the gel. It may be inferred from the comparison between C^* and CMC of sodium dodecylsulfate in pure water (8.3×10^{-3} mol l^{-1}) that CMC

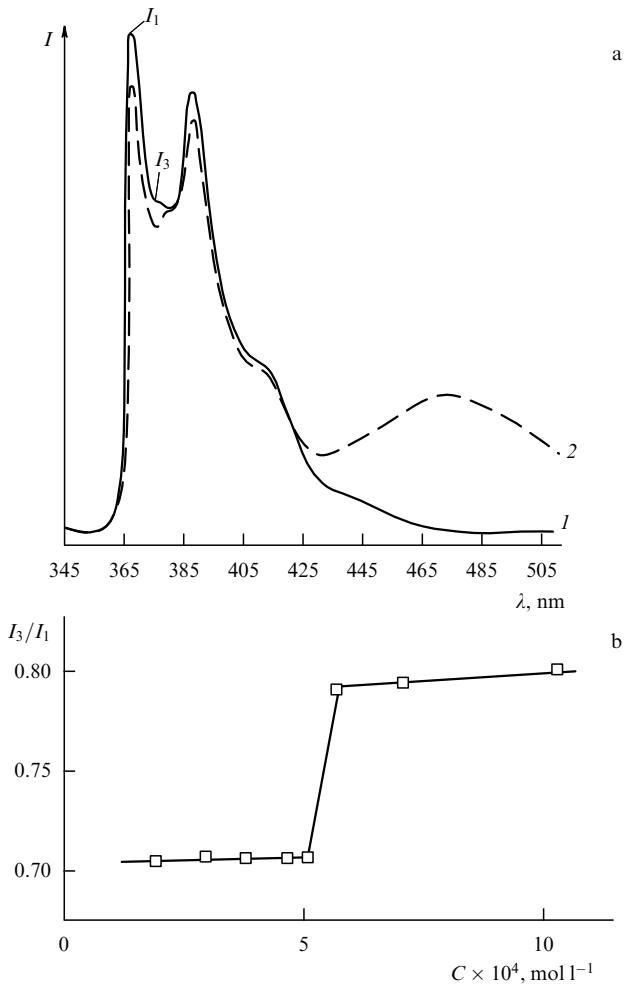

Figure 13. (a) Characteristic fluorescence spectra of pyrene molecules in aqueous (*1*) and hydrophobic (*2*) environment. Curve *2* — aqueous solution of sodium dodecylsulfate at 5.8×10^{-4} mol l^{-1}. (b) Peak intensity ratio I_3/I_1 in the pyrene fluorescence spectrum as a function of sodium dodecylsulfate concentrations in a complex with diallyldimethylammonium bromide gel.

in the gel is more than one order of magnitude lower, in excellent agreement with the theoretically predicted value [24].

It is worth noting, however, that the rise in the I_3/I_1 ratio at CMC in case of micelle formation in pure water (from 0.7 to 1.0 [55]) is much higher than for hydrophobic aggregates formed in the gel. This suggests a more polar environment of pyrene molecules absorbed by hydrophobic aggregates in the gel as compared with that of pyrene incorporated into micelles of sodium dodecylsulfate in pure water. It may be inferred that the structure of hydrophobic aggregates in the network does not coincide with the micelle structure in the solution. It was hypothesized in Ref. [49] that this is the result of incorporation of gel chains into the surfactant micellar structure inside the network.

With these findings in mind, it was natural, as the next step, to examine the structure of gel–surfactant complexes using the small-angle X-ray scattering technique. The method was employed to investigate complexes of different types [56–61], but the results proved to be very much alike. The results of the most detailed study of the structure of complexes containing cationic gels of diallyldimethylammonium chloride with sodium dodecylsulfate [58–61] are considered below.

Generally speaking, we were not prepared, in the very beginning, to find a marked regularity in the organization of micellar aggregates inside the gel, because gels are known to be products of random copolymerization of monomers and multifunctional cross-links, i.e. they are statistically disordered systems. Therefore, the results of small-angle X-ray scattering for the complex shown in Fig. 14 were surprising [58]. Intense narrow peaks of the scattering profile reflect a very high degree of order and regularity in the distribution of surfactants' aggregates inside the gel. Both the main peak and the higher-order peaks are well resolved. Their positions are indicative of the hexagonal cylindrical structure of aggregate distribution in the given complex.

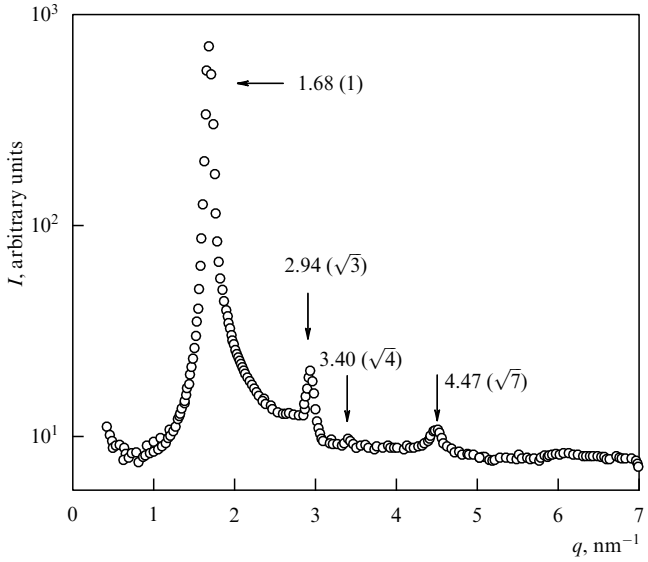

Figure 14. Intensity of small-angle X-ray scattering as a function of the scattering wave vector for a cationic diallyldimethylammonium chloride gel–anionic sodium dodecylsulfate complex.

The main peak width on the small-angle scattering curve may serve as a source of information about the degree of order of microinhomogeneities within the system. The scale over which there is practically perfect supermolecular order in the system (Fig. 14) is 80 nm, i.e. at least four times larger than the gel mesh-size. This indicates that despite the gel being a statistically disordered system, its chains must be structurally incorporated into the incipient ordered aggregates (regular microinhomogeneities). They do not disturb the order of the system which means that the medium of a statistically inhomogeneous gel is quite suitable for surfactant self-organization.

The position of the main peak determines the period of the arising structure. For the complex in Fig. 14, it is 3.7 nm, which is slightly more than the double length of sodium dodecylsulfate molecules (3.4 nm). This result is not in conflict with the fact that the gel chains may be incorporated into the arising ordered structure.

Experimental data currently available are insufficient to conclusively postulate the definite molecular structure of arising complexes, but some conjectures may be based on the experimental findings considered below [59–61]. Firstly, both the intensity and the width of the peaks depend on the

concentration of added surfactants molecules. It follows from Fig. 15a that the main peak becomes more intensive and narrow as the concentration grows; however, the peaks become broader again when the surfactant concentration exceeds CMC [60].

Furthermore, it turned out that small-angle X-ray scattering picture illustrated by Fig. 14 is not sensitive to the degree of cross-linking; that is, the wave-vector dependence of scattering intensity remains unaltered as the percentage of multifunctional units in the initial mixture varies in the range from 0.5% to 1% and 2% [59]. This result seems to indicate that cross-linking points of polymer gel chains are localized outside the regular nanostructures despite the chains themselves are involved in these ordered aggregates.

The supramolecular order of the gel-surfactant complex turned out to be very sensitive to the charge content of the gel. Figure 15b presents small-angle X-ray scattering profiles for a set of cationic gels containing 0%, 25%, 50%, 75%, and 100% of neutral acrylamide units (see Fig. 2). Evidently, the introduction of uncharged units causes a monotonic decrease in the degree of order while the corresponding characteristic spatial period slightly increases.

Finally, Ref. [60] reports small-angle X-ray scattering curves for the same cationic networks interacting not only with sodium dodecylsulfate but also with other sodium alkylsulfates differing in the length of hydrophobic tails. It turned out that the characteristic period of arising nanostructures (as deduced from the position of the main peak) grows in proportion to the length of the surfactant hydrophobic tail, as expected. The symmetry of the supercrystalline lattice being formed remains hexagonal at the hydrophobic tail length of 12, 14, and 16 carbon atoms. Sodium dodecylsulfate (10 carbon atoms) in complexes with cationic networks produces a complicated set of well-resolved narrow peaks whose positions suggest that the resultant superlattice is a simple cubic one [60].

The question arises whether the highly ordered self-organization of surfactant is an intrinsic property of gel – surfactants complexes or it can also be observed in pure aqueous solutions at the same surfactant concentration. To answer this question, small-angle X-ray scattering experiments in aqueous solutions with the same surfactant concentrations as in the gel have been performed. Figure 15c presents the results for sodium dodecylsulfate solutions at 15 and 30 weight percent. It should be emphasized that surfactant concentrations in the gel used in the experiments illustrated by Figs 14, 15 are in the same range. No signs of the highly ordered state of surfactant micelles in this concentration range were recorded. Therefore, the degree of molecular ordering in a network is higher than in aqueous solutions at equal surfactant concentrations notwithstanding the statistically disorded gel nature. This means that the medium of a statistic polyelectrolyte gel facilitates the formation of perfect nanostructures of oppositely-charged surfactant rather than hampering it.

This fact may have far-reaching consequences for the development of new techniques to produce substances with the predetermined microstructure. Perfect molecular structures have until recently been prepared using the self-assembly procedure on surfaces [62, 63]. However, this approach does not solve all potential problems because the presence of a surface inevitably introduces the plane layer motif into the resulting structures. Polymer gels may serve as alternative matrices for self-assembly which allow molecular organization to be realized in the gel volume rather than in the plane. Naturally, further progress in this field depends on the ability to prepare networks of controlled topological structure, which is a non-trivial problem.

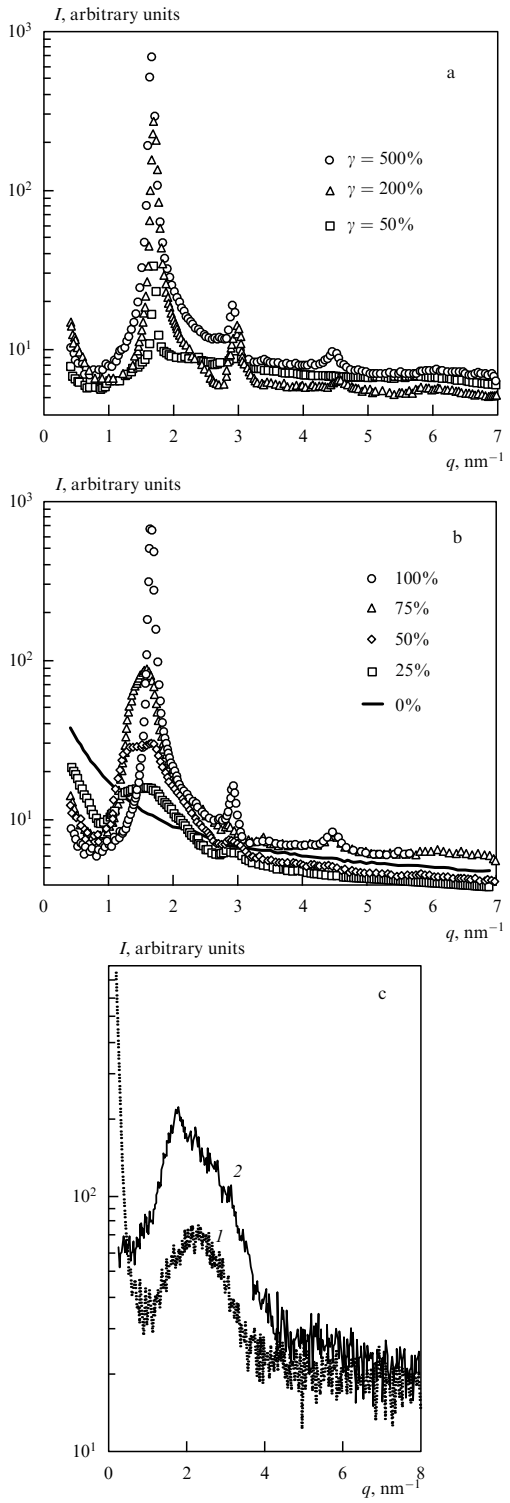

Figure 15. (a) Small-angle X-ray scattering curves for diallyldimethylammonium chloride gels – sodium dodecylsulfate complexes at different molar ratios of the number of added surfactant molecules to that of charged monomer units of the network. (b) Small-angle X-ray scattering curves for diallyldimethylammomium chloride – acrylamide copolymer gels interacting with sodium dodecylsulfate. (c) Small-angle X-ray scattering curves for 15 (*1*) and 30 (*2*) weight percent aqueous solutions of sodium dodecylsulfate at room temperature.

5. The multiplet structure in ionomer systems

It has been noted in the Introduction that the situation when counterions dissociate and move independently of the polyelectrolyte chains is not unique. In a low-polarity medium (an organic liquid instead of water, or ion-containing polymer melts), counterions 'condense' on the ions of the polymer chain forming the so-called ion pairs (Fig. 1b). The ion pair concept applies to weakly charged systems in which point charges associate (see, for instance, Fig. 1b). The resultant macromolecule with ion pairs widely spaced along the chain is called ionomer [64]. In case of strongly charged polymer chains, condensation of counterions occurs along the charged line, i.e. at an object with cylindrical symmetry. The latter case is worth special consideration and lies beyond the scope of the present review, having been examined in a number of other reports [65, 66].

Turning back to ionomers, i.e. weakly charged polyelectrolytes with condensed counterions (Fig. 1b), let us consider conditions for the thermodynamically advantageous formation of ion pairs. Association of two opposite charges into an ion pair results in saving Coulomb energy of $e^2/\varepsilon r_0$, where e is the elementary charge, ε is the dielectric constant of the medium, and r_0 is the intercharge distance in the ion pair. Simultaneously, one of the ions loses translational entropy; the loss to the logarithmic factor accuracy is kT per one ion pair. Therefore, it appears that ion pair formation (Fig. 1b) is favorable when the dimensionless parameter $u \equiv e^2/\varepsilon r_0 kT$ exceeds unity, whereas free counterions prevail at $u < 1$ (Fig. 1a). For this reason, the system is in the polyelectrolyte regime at $u < 1$ and in the ionomeric regime at $u > 1$. As follows from the expression for u, the ionomeric regime is realized at relatively low dielectric constants of the medium. Substituting the table values of e, k and $r_0 \sim 0.7$ nm, it is easy to see that at room temperature the boundary value of e is about 50. The polyelectrolyte regime is realized in more polar media (e.g. aqueous solutions) while the ionomeric regime corresponds to low-polar milieu. So, the latter regime is realized for polymer melts due to the normally low polarity of uncharged monomer units.

The present section concerns the self-organization in ionomer melts. Let us consider a melt of a chains (like that in Fig. 1b), whose uncharged units do not specifically interact with one another or with ion pairs. Then, the ion pairs are the only interacting centers due to dipole-dipole forces acting between them. This interaction appears to be of attractive nature because it is always possible to ensure the desired reciprocal orientation of dipoles in a melt of flexible polymer chains. Therefore, from the standpoint of statistical physics, the ionomer chain can be considered as a statistical A – B copolymer with sparse strongly attractive B-units (Fig. 16a). What can be the structure of such melts? Evidently, B-attractors are likely to aggregate, the aggregation number, however, is limited for steric reasons. Hence, there is a structure like that shown in Fig. 16b. In polymer physics, ion pair aggregates are called multiplets and the resultant structure is known as a multiplet one [67].

Our approach to the theoretical description of multiplet structures in ionomer melts [68 – 71] is based on the analogy between formation of such structures and microphase separation in block-copolymers [31 – 33]. Indeed, if we had short B-blocks instead of individual B-units in Fig. 16a, the melt of such block-polymers would contain spherical B-micelles surrounded by the 'sea' of A-chains. In other words, the situation will be analogous to that presented in Fig. 16b. Microphase separation in block-copolymers has been investigated in many papers [31 – 33, 72, 73], and the approaches to its theoretical description are well known. The key idea of our study [68] was to apply them to the description of the structure of a block-copolymer melt and to consider the limit when the length of the B-block tends to unity. However, it turned out that there is no straightforward realization of this idea.

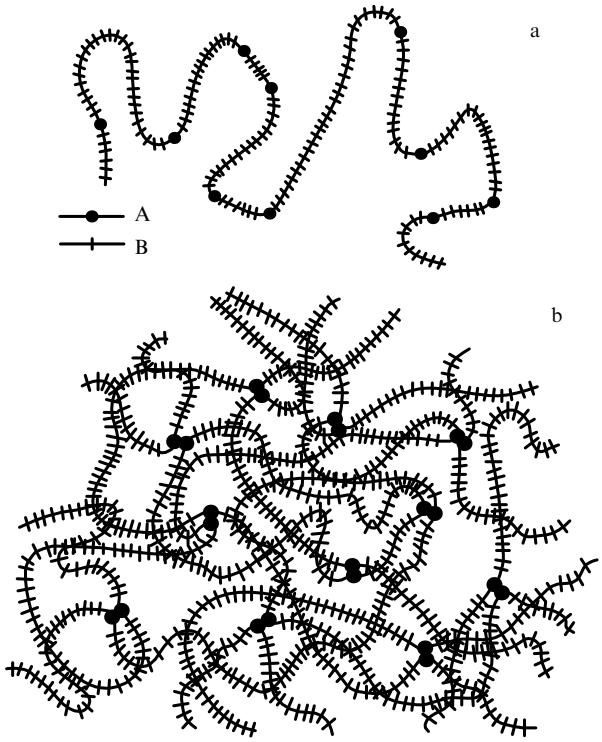

Figure 16. (a) Statistical copolymer with sparse strongly attracting B-units: ionomer chain model; (b) multiplet structure in an ionomer melt.

Let us consider an isolated micelle (Fig. 17). Let the number of units in chain B be N_B (this value will further be tended to unity in order to pass onto the ionomer case), that in chain A be N_A, and the coefficient of surface tension between A and B media be σ. Strong aggregation of the components is assumed, as it takes place between ion pairs and the non-polar A-environment. To obtain the characteristics of B-micelles (the radius R_B and the aggregation number Q, i.e. the number of B-blocks per micelle), let us consider first the free energy which can be written as the sum of three contributions [68]:

$$F = F_1 + F_2 + F_3 , \tag{5}$$

where $F_1 = 4\pi R_B^2 \sigma$ is the surface free energy, F_2 is the free energy of A-block stretching in the micellar 'corona', and F_3 is the free energy of B-chain stretching in the micellar core (it can be shown that the chains are actually stretched there). The F_2 and F_3 contributions can be calculated by standard methods, well known from the theory of block-copolymers. It has been shown [68] that

$$F_2 = \frac{3}{2\pi} \frac{kT}{R_B} Q^2 , \qquad F_3 = \frac{3\pi^2}{80} kT \frac{R^2}{N_B l_B^2} , \tag{6}$$

where l_B is the length of the Kuhn segment of B-chain. For simplicity, the chains A and B are supposed to be identical in

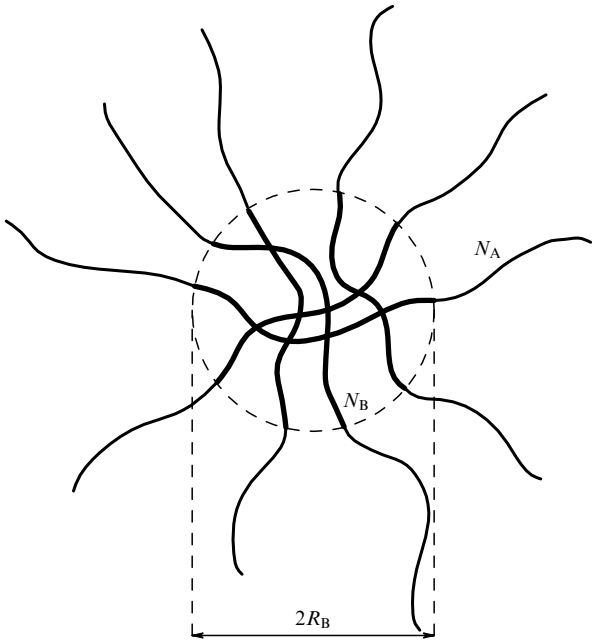

Figure 17. Isolated spherical B-micelle.

terms of elasticity and excluded volume, that is to have similar geometries and lengths of Kuhn segments. The free energy (5) must be minimized over Q taking into account the obvious condition

$$R_B = \left(\frac{3}{4\pi} Q v N_B\right)^{1/3}, \tag{7}$$

where v is the volume of a monomer unit (A or B). For flexible A and B chains, $v \sim a^3$, $l_B \sim a$ [4]. Bearing this in mind, minimization of the expression (5) gives the following expressions for the aggregation number and the radius of B-micelle

$$Q \simeq \frac{\sigma a^2}{kT} N_B, \qquad R \simeq \left(\frac{\sigma a^2}{kT} N_B^2\right)^{1/3} a. \tag{8}$$

However, the analysis of expressions (8) has shown that they cannot be valid for very large degrees of incompatibility between the components (i.e. at large σ values). This case is of special interest for us as far as the description of multiplet structures in ionomers is concerned. Indeed, at

$$\frac{\sigma a^2}{kT} > N_B \tag{9}$$

the second expression in (8) gives $R_B > N_B a$ which suggests that the micelle size is larger than the length of the completely stretched B-chain, which is certainly out of the question. Similar difficulties are encountered [if inequality (9) is fulfilled] as regards location of junction points of chains A and B at the micelle surface.

Analysis of this problem in Ref. [68] suggested that the system shifts to a new regime (provided the condition (9) is satisfied) which has never been considered in the theory of block- polymers. It was called the superstrong segregation regime. In this regime, the aggregation number and the radius of B-micelles are defined by the following relations [instead of expressions (8)]:

$$Q \cong N_B^2, \qquad R_B \cong a N_B, \tag{10}$$

meaning that the chains in B-micelles are close to their extensibility limit, while their entire surfaces are covered by junction points between A and B chains.

Now, let us turn to ionomer melt (Fig. 16b) and examine the limit $N_B \to 1$ for the case of strong incompatibility between the components. Certainly, the inequality (9) is always satisfied in this case. Therefore, it is inferred that the block-copolymer regime similar to that for ionomer multiplets is actually the superstrong segregation regime. The transition to the $N_B \to 1$ limit for the description of the multiplet structure in an ionomer melt should certainly be done in the framework of this regime.

This conclusion, first made in Ref. [68], allowed analyzing theoretically the multiplet structure (Fig. 16 b). Here are some of the results. The aggregation number for statistical ionomers (of the type shown in Fig. 16a) turned out to be about 8 times smaller than that for telechelic ionomers (macromolecular chains having ion pairs only at their ends). This conclusion is in good agreement with experimental data [74]. Moreover, the mean square radius of gyration of ionomer chains in the melt proved to be larger than the unperturbed radii, due to considerable A-chain extension near the multiplet (see Fig. 17). This also accounts for the presence of two experimentally found glass temperatures in ionomer melts [75]; firstly, the strongly elongated in the vicinity of multiplets

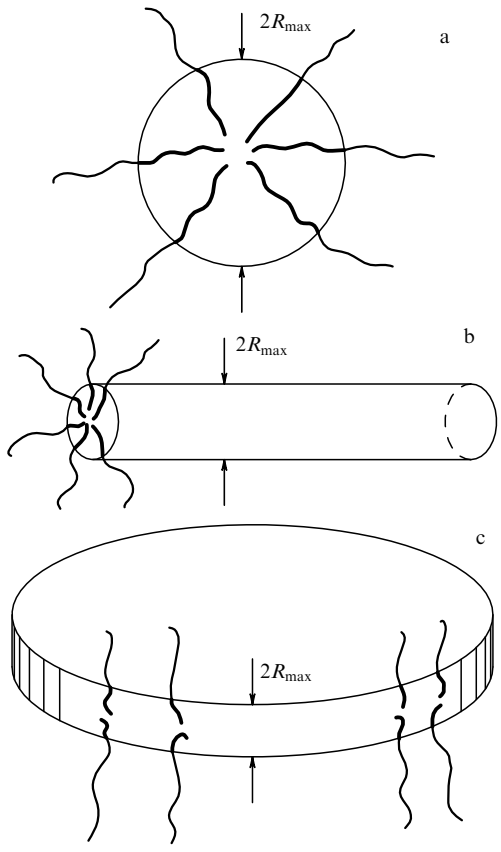

Figure 18. Spherical (a), cylindrical (b), and disk-like (lamellar) (c) B-micelles in the superstrong segregation limit.

A-chains are solidified, followed by the remaining regions. Finally, the average distance between adjacent multiplets in an ionomer melt is smaller than the mean square radius of gyration of the A-chain between two multiplets [68]. This means that A-chains largely connect multiplets which are not immediate neighbors in the space.

The question is whether the superstrong segregation regime is only realizable for ionomers like those in Fig. 1b, or it is equally possible in block-copolymer systems. For this regime to be realized, the condition (9) must be fulfilled. Now, this condition does not hold when B-blocks are sufficiently long. However, the superstrong segregation regime can be probably realized if B-blocks are oligomers ($N_B \lesssim 20$) and the components are strongly incompatible. This inference has been confirmed in experiments with block-ionomers having relatively short ionomer and long non-polar blocks [76, 77]. Specifically, these studies have demonstrated that aggregation numbers for short ionomeric blocks are unusually large compared with those for ordinary block-copolymers under similar conditions, the chains in ionomer micelles are almost completely stretched, i.e. the radius of a B-micelle is proportional to N_B rather than to $N_B^{2/3}$ as in the block-copolymer case [see Eqn (8)]. This anomality disappears as the B-block becomes longer. These results are in excellent agreement with the above theory describing the superstrong segregation regime.

Now, let us study the thermodynamically optimal shape of multiplets in the superstrong segregation regime. In principle, it follows from the above reasoning that B chains in micelles must be extended regardless of the micelle shape, which can be spherical, cylindrical or lamellar (Fig. 18). The problem of the optimal shape of micelles in the limit of very large A – B surface energy can be resolved from the following simple considerations. Figure 18 shows that the surface free energy per B-block in a spherical micelle is

$$\frac{F_{int}}{Q} \simeq \frac{\sigma}{kT} \frac{4\pi R_B^2}{4\pi R_B^3/3} N_B v \simeq 6 \frac{\sigma}{kT} \frac{v}{a}, \qquad (11)$$

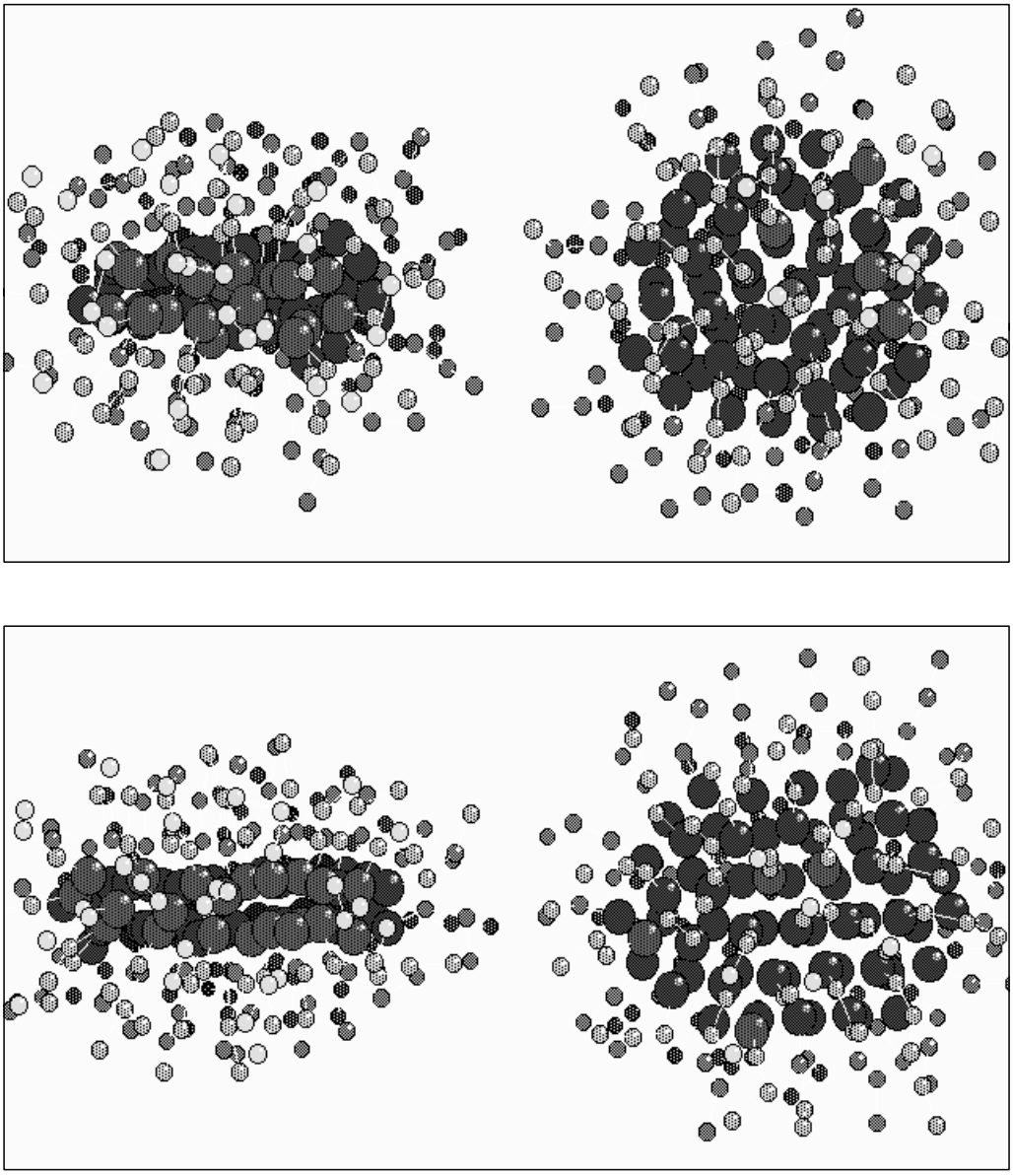

Figure 19. Typical snapshots of three-dimensional micelles viewed from two mutually perpendicular directions in the system of 128 four-unit chains with strongly interacting end-groups.

in a cylindrical micelle of length l

$$\frac{F_{\text{int}}}{Q} \simeq \frac{\sigma}{kT}\frac{2\pi R_{\text{B}} l}{\pi R_{\text{B}}^2} N_{\text{B}} v \simeq 4\,\frac{\sigma}{kT}\frac{v}{a}\,, \tag{12}$$

and in a lamella (a thin disk-like B-layer with diameter D)

$$\frac{F_{\text{int}}}{Q} \simeq \frac{\sigma}{kT}\frac{\pi D^2/4}{\pi D^2 R_{\text{B}}/4} N_{\text{B}} v \simeq 2\,\frac{\sigma}{kT}\frac{v}{a}\,. \tag{13}$$

It is clear that the expression (13) gives the minimal value of the surface free energy. On the other hand, this contribution to the free energy must be predominant in the limit of very large σ (i.e. in the superstrong segregation regime). Therefore, it is lamellar (or disk-like) micelles that are thermodynamically stable in the superstrong segregation limit. This result was first obtained in Ref. [69].

A more detailed analysis in Ref. [69] has demonstrated that disk-like micelles (multiplets) of a finite diameter are always (at reasonable values of parameters) more favorable than an infinite micellar layer. It is accounted for by the corrections to the main term of the free energy (13). They are of order R_{B}/D , resulting from the surface energy of disk edges and the chain stretching energy in the A-corona of the disk. The results reported in Ref. [69] may be more accurately described in the following way. A change in the shape of B-micelles from spherical to disk-like occurs at the critical value of surface energy

$$\frac{\sigma^* a^2}{kT} = \frac{1}{6}\,N_{\text{B}} \tag{14}$$

and is in fact the continuous phase transition of the second order. At $\sigma > \sigma^*$, there is superstrong segregation regime in which micelles (multiplets) are disk-like formations, and their diameter D is defined by the relation

$$D = R_{\text{B}}\left[1 + \frac{2}{3}\left(\sqrt{\frac{\sigma}{\sigma^*}} - 1\right)\right]. \tag{15}$$

When σ values are very large, starting from

$$\frac{\sigma^{**} a^2}{kT} = \frac{3N_{\text{A}}^2}{2\pi N_{\text{B}}^2}$$

(such values are not likely to be realized in experiment), the first order phase transition occurs from the disk-like micelle to infinite lamella.

The finding that the disk-like form of B-micelles (hence, of ionomer multiplets) corresponds to thermodynamic equilibrium in the superstrong segregation limit has been verified in Refs [78, 79] by the molecular dynamics method for the simplest chain models for which this regime is feasible, namely, for short chains with strongly attracting functional end-groups. It turned out in the course of the study that the equilibrium micellar shape is difficult to obtain because the system tends to generate randomly oriented frozen structures (see below). Therefore, a special method to prepare stable micelles was suggested. The initially large radius of attraction was chosen (to avoid formation of frozen structures) which was further gradually reduced to realistic values. The result is presented in Fig. 19: the 'snapshots' of micelles viewed from two mutually perpendicular directions confirm their disk-like geometry. This finding is supported by a monotonic increase in the mean square radius of gyration of the micellar core with decrease of radius of interaction between functional groups r_{c} [78, 79]. It is worth noting that a further decrease in r_{c} leads to disintegration of a disk-like micelle into two disks.

If no precaution is taken to ensure the equilibrium structure, the system is rapidly 'frozen' due to the strong attraction between functional groups in randomly formed aggregates (multiplets). A typical model example for two-dimensional case is presented in Fig. 20. The aggregates resulting from strong end-group interactions have little in common with a disk or other elongated objects. At the same time, the calculated statistical structural factor of scattering from functional groups in Fig. 20 gives a curve with the prominent peak corresponding to the average distance between multiplets. Thus, a certain structural organization persists in this case too.

The results presented in this section indicate that ionomer melts tend to be self-organized in a variety of ways. Similar structures can be found in ionomer solutions in organic solvents. Disk-like multiplets have the most important practical implications since they impart a structural motif for conducting planes in organic matrices. However, it should be borne in mind that ionomers, like other polymers with strongly associated groups, exhibit the tendency to form kinetically frozen structures due to the strong interaction

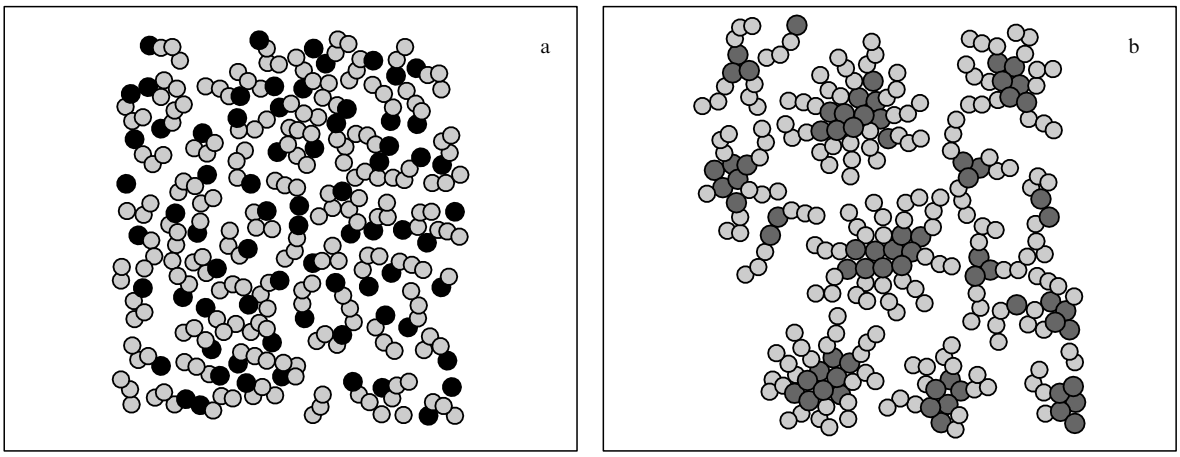

Figure 20. Two-dimensional system of four-unit chains with strongly attracting end-groups. (a) initial configuration (prior to interaction), (b) kinetically frozen multiplet structure after the initialization of interaction.

between ion pairs. Such structures may upset thermodynamically-driven self-organization.

6. Conclusion

The present review is confined to a few examples of self-organization in ion-containing polymer systems. It does not cover effects of mixed polyelectrolyte–ionomer behavior [80–83], self-organization of block-copolymers with one polyelectrolyte and one hydrophobic component [84, 85], ordering in gel–linear polymer complexes [25, 26], copolymerization of certain types of polyelectrolyte macromolecules, e.g. DNA, during collapse [86–88], and other issues.

For all that, the above examples appear sufficient to illustrate highly variable patterns of self-organization in ion-containing polymer systems due to the competition between different types of interactions. Taken together, high susceptibility of such systems to external impacts, a great variety of structural motifs for the molecular architecture, and ample opportunity for the managed self-assembly in the volume, make the research on the formation of nanostructures in ion-containing polymers one of the most interesting and practically important aspects of the modern science of polymers.

References

1. Lifshits I M *Zh. Eksp. Teor. Fiz.* **55** 2408 (1968) [*Sov. Phys. JETP* **28** 1280 (1969)]
2. Lifshits I M, Grosberg A Yu *Zh. Eksp. Teor. Fiz.* **65** 2399 (1973) [*Sov. Phys. JETP* **38** 1198 (1974)]
3. Lifshitz I M, Grosberg A Yu, Khokhlov A R *Rev. Mod. Phys.* **50** 683 (1978)
4. Lifshits I M, Grosberg A Yu, Khokhlov A R *Usp. Fiz. Nauk* **127** 353 (1979) [*Sov. Phys. Usp.* **22** 123 (1979)]
5. Lifshits I M, Grosberg A Yu, Khokhlov A R *Perekhody Klubok–Globula v Polimernykh Sistemakh* (Coil–Globule Transition in Polymer Systems) (Pushchino: NTsBI, 1981)
6. Khokhlov A R *J. Phys. A* **13** 979 (1980)
7. Khokhlov A R *Polymer* **21** 376 (1980)
8. Khokhlov A R *Vysokomol. Soedin. A* **22** 737 (1980) [*Polym. Sci. USSR A*]
9. Khokhlov A R, Khachaturian K A *Polymer* **23** 1742 (1982)
10. Khokhlov A R, Vasilevskaya V V, in *Matematicheskie Metody dlya Issledovaniya Polimerov* (Mathematical Methods in Polymer Studies) (Eds I M Lifshits, A M Molchanov) (Pushchino: NTsBI, 1982) p. 45
11. Vol'kenshteĭn M V *Molekulyarnaya Biofizika* (Molecular Biophysics) (Moscow: Nauka, 1981)
12. Ben-Naim A, in *Hydrophobic Interaction* (New York: Plenum Press, 1980)
13. Tanford C, in *The Hydrophobic Effect: Formation of Micelles and Biological Membranes* (New York: Wiley, 1973)
14. Tanaka T et al. *Phys. Rev. Lett.* **45** 1636 (1980)
15. Grosberg A Yu, Khokhlov A R *Statisticheskaya Fizika Makromolekul* (Statistical Physics of Macromolecules) (Moscow: Nauka, 1989)
16. Dusek K, Prins W *Adv. Polym. Sci.* **6** 1 (1969)
17. Tanaka T *Phys. Rev. Lett.* **40** 820 (1978)
18. Ilavsky M *Macromolecules* **15** 782 (1982)
19. Khokhlov A R, Starodubtzev S G, Vasilevskaya V V *Adv. Polym. Sci.* **109** 123 (1993)
20. Tanaka T, Shibayama M *Adv. Polym. Sci.* **109** 1 (1993)
21. Ohmine I, Tanaka T *J. Chem. Phys.* **77** 5725 (1982)
22. Vasilevskaya V V, Khokhlov A R *Vysokomol. Soedin. A* **28** 316 (1986) [*Polym. Sci. USSR A*]
23. Khokhlov A R et al. *Macromolecules* **25** 4779 (1992)
24. Khokhlov A R et al. *Makromol. Chem. Theory Simul.* **1** 105 (1992)
25. Khokhlov A R, Vasilevskaya V V *Macromolecules* **25** 2398 (1994)
26. Philippova O E, Karibyants N S, Starodubtzev S G *Macromolecules* **27** 2398 (1994)
27. Tanaka T, Sun S T, Nishio I, in *Scattering Techniques in the Application to Supramolecular and Nonequilibrium Systems* (*Proc. NATO Adv. Study Inst.*) **73** 321 (1981)
28. Hirokawa Y, Tanaka T *J. Chem. Phys.* **81** 6379 (1985)
29. Makhaeva E E et al. *Macromol. Chem. Phys.* **197** 1973 (1996)
30. Shibayama M, Tanaka T, Han C C *J. Chem. Phys.* **97** 6842 (1992)
31. Leibler L *Macromolecules* **13** 1602 (1980)
32. Erukhimovich I Ya *Vysokomol. Soedin. A* **24** 1942 (1982) [*Polym. Sci. USSR A* **24** 2223 (1983)]
33. Semenov A N *Zh. Eksp. Teor. Fiz.* **88** 1242 (1985) [*Sov. Phys. JETP* **61** 733 (1985)]
34. Schosseler F, Ilmain F, Candau S J *Macromolecules* **24** 225 (1991)
35. Moussaid A et al. *J. de Phys. II* **3** 573 (1993)
36. Boryu V Yu, Erukhimovich I Ya *Dokl. Akad. Nauk SSSR* **286** 1373 (1986) [*Sov. Phys. Dokl.* **31** 146 (1986)]
37. Boru V Yu, Erukhimovich I Ya *Macromolecules* **21** 3240 (1988)
38. Khokhlov A R, Nyrkova I A *Macromolecules* **25** 1493 (1992)
39. Dobrynin A V, Erukhimovich I Ya *Zh. Eksp. Teor. Fiz.* **99** 1344 (1991) [*Sov. Phys. JETP* **72** 751 (1991)]
40. Nyrkova I A, Khokhlov A R, Kramarenko E Yu *Vysokomol. Soedin. A* **32** 918 (1990) [*Polym. Sci. USSR* **32** 852 (1990)]
41. Nyrkova I A, Khokhlov A R, Doi M *Macromolecules* **27** 4220 (1994)
42. Dormidontova E E, Erukhimovich I Ya, Khokhlov A R *Macromol. Theory Simul.* **3** 661 (1994)
43. Flory P *Principles in Polymer Chemistry* (Ithaca: Cornell Univ. Press, 1953)
44. Landau L D, Lifshitz I M *Statisticheskaya Fizika* (Statistical Physics) (Moscow: Nauka, 1976) [Translated into English 2 Vols, 3rd edition (Oxford: Pergamon Press, 1980)]
45. Zeldovich K B, Dormidontova E E, Khokhlov A R *J. de Phys. II* (April 1997)
46. de Gennes P G *J. de Phys. Lett.* **40** L-69 (1979)
47. Annaka M, Tanaka T *Nature* **355** 430 (1992)
48. Starodubtsev S G, Ryabina V R, Khokhlov A R *Vysokomol. Soedin. A* **32** 969 (1990) [*Polym. Sci. USSR A*]
49. Philippova O E, Starodubtzev S G *J. Polym. Sci. B* **31** 1471 (1993)
50. Makhaeva E E, Starodubtzev S G *Makromol. Chem. Rap. Commun.* **14** 105 (1993)
51. Makhaeva E E, Starodubtzev S G *Polym.Bull.* **30** 327 (1993)
52. Starodubtzev S G et al. *Macromol. Chem. Phys.* **196** 1855 (1995)
53. Philippova O E et al. *Macromolecules* **29** 2822 (1996)
54. Tkhan' L M, Makhaeva E E, Starodubtsev S G *Vysokomol. Soedin. A* **35** 408 (1993) [*Polym. Sci. USSR A*]
55. Filippova O E, Makhaeva E E, Starodubtsev S G *Vysokomol. Soedin. A* **34** 82 (1992) [*Polym. Sci. A*]
56. Khandurina Yu V et al. *Vysokomol. Soedin. A* **36** 255 (1994) [*Polym. Sci. A*]
57. Okuzaki H, Osada Y *Macromolecules* **28** 380 (1995)
58. Chu B et al. *Macromolecules* **28** 8447 (1995)
59. Yeh F et al. *J. Am. Chem. Soc.* **118** 6615 (1996)
60. Sokolov E L, Khokhlov A R, Chu B *Langmuir* (1996) (in press)
61. Dembo A T et al. *J. Polym. Sci. B* (1997) (in press)
62. Lehn J M *Supramolecular Chemistry* (Oxford: Oxford Univ. Press, 1994)
63. Lvov Y et al. *J. Am. Chem. Soc.* **117** 6117 (1995)
64. Schlick S (Ed.) *Ionomers: Characterization, Theory and Applications* (New York: CRC Press, 1996)
65. Manning G S *J. Chem. Phys.* **51** 924 (1969)
66. Manning G S *Q. Rev. Biophys.* **11** 179 (1978)
67. Eisenberg A *Macromolecules* **3** 147 (1970)
68. Nyrkova I A, Khokhlov A R, Doi M *Macromolecules* **26** 3601 (1993)
69. Semenov A N, Nyrkova I A, Khokhlov A R *Macromolecules* **28** 7491 (1995)
70. Semenov A N, Joanny J F, Khokhlov A R *Macromolecules* **28** 1066 (1995)
71. Semenov A N, Nyrkova I A, Khokhlov A R, in *Ionomers: Characterization, Theory and Applications* (Ed. S Schlick) (New York: CRC Press, 1996) p. 251
72. Bates F, Fredrickson G H *Ann. Rev. Phys. Chem.* **41** 525 (1990)
73. Binder K *Adv. Polym. Sci.* **112** 181 (1994)
74. Williams C E, in *Multiphase Macromolecular Systems* (Ed. B M Culberston) (New York: Plenum Press, 1989)
75. Eisenberg A, Hird B, Moore R *Macromolecules* **23** 4098 (1990)

76. Earnest T R et al. *Macromolecules* **14** 192 (1981)
77. Forsman W C, MacKnight W J, Higgins J S *Macromolecules* **17** 490 (1984)
78. Khalatur P G et al. *Macromol. Theory Simul.* **5** 713 (1996)
79. Khalatur P G et al. *Macromol. Theory Simul.* **5** 749 (1996)
80. Khokhlov A R, Kramarenko E Yu *Macromol. Theory Simul.* **3** 45 (1994)
81. Starodubtsev S G et al. *Macromolecules* **28** 3930 (1995)
82. Khokhlov A R, Kramarenko E Yu *Macromolecules* **29** 681 (1996)
83. Philippova O E et al. *Macromolecules* (1996) (in press)
84. Zhulina E B *Macromolecules* **26** 6273 (1993)
85. Shusharina N P, Nyrkova I A, Khokhlov A R *Macromolecules* **29** 3167 (1996)
86. Minagawa K et al. *Biopolymers* **34** 555 (1994)
87. Vasilevskaya V V et al. *J. Chem. Phys.* **102** 6595 (1995)
88. Yoshikawa K et al. *Phys. Rev. Lett.* **76** 3029 (1996) 235 (1994)